

# Observation of standard spin-switch effects in F/S/F trilayers with a strong ferromagnet

Ion C. Moraru, W. P. Pratt, Jr., Norman O. Birge\*

Department of Physics and Astronomy, Michigan State University, East Lansing, Michigan 48824-2320, USA

(Dated: March 23, 2022)

We have measured the superconducting transition temperature  $T_c$  of F/S/F trilayers using Permalloy (Py= $\text{Ni}_{84}\text{Fe}_{16}$ ) as a strongly polarized ferromagnetic material. For a parallel (P) or anti-parallel (AP) alignment of the magnetization directions of the outer ferromagnets, we observe a  $T_c$  difference as large as 20 mK, with a stronger suppression of superconductivity in the P state than in the AP state. This behavior is opposite to the recent observations of Rusanov *et al.*, Phys. Rev. B **73**, 060505 (2006) in Py/Nb/Py trilayers, but is consistent with earlier results on trilayers with Ni or CuNi alloy as the ferromagnetic material.

PACS numbers: 74.45.+c, 85.75.-d, 85.25.-j, 73.43.Qt

The presence of a ferromagnetic (F) material in contact with a conventional superconductor (S) results in a strong mutual influence.<sup>1</sup> The superconducting correlations penetrate into the ferromagnet and oscillate in sign over a very short distance, due to the large energy difference between the majority and minority spin bands in the ferromagnet. Bilayers, trilayers, and multilayers of S and F materials exhibit a wide variety of novel phenomena, including oscillations of the superconducting critical temperature<sup>2,3,4</sup> and density of states<sup>5</sup>, and Josephson junctions with a  $\pi$ -shifted ground state.<sup>6</sup>

In this paper we focus on the so-called “superconducting spin switch” first discussed in 1966 by deGennes<sup>7</sup> and rediscovered in 1999 by Tagirov<sup>8</sup> and by Buzdin, Vedyayev and Ryzhanova.<sup>9</sup> Those authors predicted that the critical temperature,  $T_c$ , of a F/S/F trilayer should depend on the relative magnetization direction of the two F layers, with the smallest  $T_c$  occurring in the parallel (P) state and the largest  $T_c$  in the antiparallel (AP) state. Those predictions were verified long ago by Deutscher and Meunier,<sup>10</sup> and more recently by Gu *et al.*,<sup>11</sup> Potenza and Marrows,<sup>12</sup> and Moraru *et al.*<sup>13</sup> in a variety of F/S/F systems. It came as a surprise, therefore, when Rusanov *et al.*<sup>14</sup> recently reported observation of the *inverse* spin switch effect in a series of Py/Nb/Py trilayer samples. Although the difference in  $T_c$  between the P and AP magnetization configurations was small in that work, the data showed clearly that the resistance in the transition region was higher for the AP configuration than for the P one. In fact, similar behavior had previously been observed by Peña *et al.*<sup>15</sup> in F/S/F trilayers made from superconducting  $\text{YBa}_2\text{Cu}_3\text{O}_4$  and ferromagnetic  $\text{La}_{0.7}\text{Ca}_{0.3}\text{MnO}_3$ , with a spin polarization expected to be close to 100%. Those authors interpreted their observations as arising from enhanced reflection of spin-polarized quasiparticles at the F/S interfaces in the AP state leading to a stronger suppression of superconductivity,<sup>16</sup> and Rusanov *et al.*<sup>14</sup> claimed that the inverse spin-switch behavior is generic for F/S/F trilayers with strong ferromagnets. We believe that the mechanism based on reflection of quasiparticles at the S/F interface<sup>16</sup> can explain changes in resistance under

nonequilibrium conditions, but cannot explain differences in the equilibrium  $T_c$  between the P and AP states. Given our earlier work showing standard spin-switch behavior in Ni/Nb/Ni trilayers,<sup>13</sup> we were motivated to carry out independent measurements of  $T_c$  in Py/Nb/Py trilayers.

A series of  $\text{Py}(8)/\text{Nb}(d_s)/\text{Py}(8)/\text{Fe}_{50}\text{Mn}_{50}(8)/\text{Nb}(2)$  multilayers (all thicknesses are in nm) was fabricated, with thicknesses for the superconducting layer,  $d_s$ , varying between 20 and 150 nm. The samples were grown directly onto Si substrates by magnetically-enhanced triode dc sputtering in a high vacuum chamber with a base pressure in the low  $10^{-8}$  Torr and an Ar pressure of  $2.0 \cdot 10^{-3}$  Torr. The thickness of the Py layers were chosen to be much longer than the dirty-limit coherence length,  $\sqrt{\hbar D_F^\uparrow / E_{ex}}$ , which we estimate to be 1.2 nm for the majority spin band using  $E_{ex} = 0.135$  eV,<sup>17</sup>  $D_F^\uparrow = v_F^\uparrow l_F^\uparrow / 3$ ,  $v_F^\uparrow = 0.22 \cdot 10^6$  m/s and  $l_F^\uparrow = 4$  nm.<sup>18</sup> The FeMn layer fixes the direction of the top Py layer by exchange bias<sup>20</sup> after undergoing a brief annealing and in-field cooling process. The Nb capping layer protects the FeMn from oxidation and is not superconducting.

Samples were patterned for four-terminal current-in-plane resistance measurements by mechanical masking during sputtering. The lateral dimensions of the samples were 4.3 mm x 1.6 mm. The critical temperatures of all samples were determined by ac resistance measurements with current of 10  $\mu\text{A}$ , corresponding to a current density less than  $3 \times 10^5$  A/m<sup>2</sup>, low enough to be in the linear response regime.  $T_c$  was defined to be the temperature at which the resistance dropped to half its normal state value.

The results for the  $T_c$  measurements are summarized in Fig. 1. The  $T_c$  of the trilayer shows a strong dependence on the superconductor thickness close to a critical thickness,  $d_s^{cr}$ , where the sensitivity to ferromagnetism is enhanced. No superconductivity is observed above 36 mK for  $d_s < d_s^{cr} \approx 20.5$  nm.

We have verified the magnetic configuration of our structures on simultaneously sputtered samples of larger lateral size using a SQUID magnetometer. Fig. 2 shows a plot of magnetization vs. applied field,  $H$ , for a sample



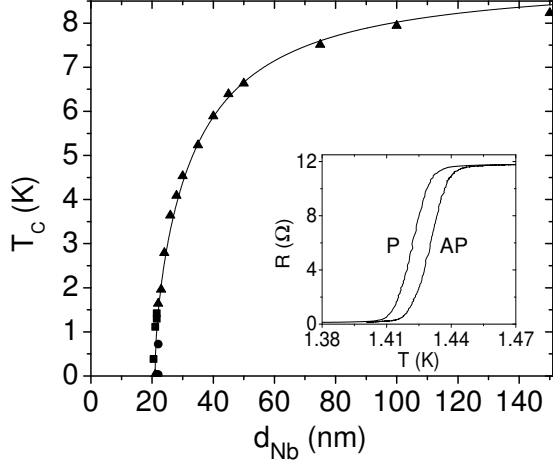


FIG. 1: Critical temperature vs. Nb thickness for a series of  $\text{Py}(8)/\text{Nb}(d_s)/\text{Py}(8)/\text{Fe}_{50}\text{Mn}_{50}(8)/\text{Nb}(2)$  samples (all thicknesses are in nm). The various symbols represent different sputtering runs. The solid line represents the theoretical fit as explained in the text. Inset:  $R$  vs.  $T$  for a  $d_s=21.5$  nm sample illustrating the difference between  $T_c$  for the P and AP states.

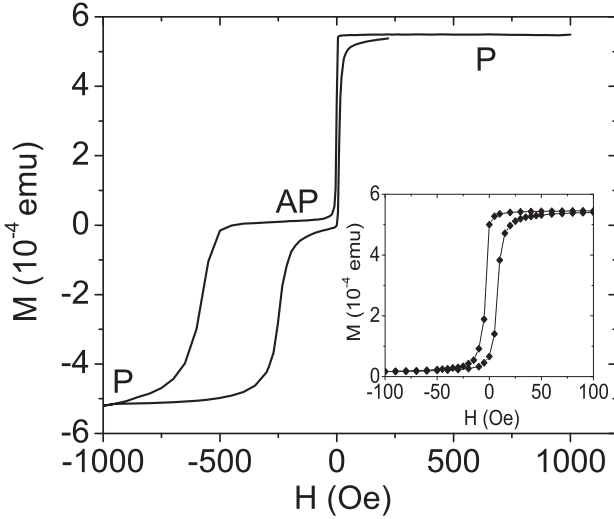


FIG. 2: Magnetization vs. applied field for a  $d_s = 23$  nm sample measured at  $T = 4.2$  K. At  $H \approx \pm 10$  Oe the free bottom Py layer switches while the pinned top Py layer switches at around -500 Oe. Inset: minor loop measured at  $T = 4.2$  K showing good switching of the free Py layer.

with  $d_s = 23$  nm taken at 4.2 K, illustrating the typical spin-valve behavior of the trilayer. The narrow hysteresis loop near  $H = 0$  shows the switching of the free Py layer with a coercive field  $H_c = 5 - 10$  Oe, while the wider loop shows switching of the pinned layer, shifted to nonzero  $H$  due to the exchange bias with the FeMn.

The inset to Fig. 2 shows a minor hysteresis loop illustrating that applied fields of  $\pm 100$  Oe switch the trilayer fully between the P and AP configurations. The nearly zero net magnetization observed at -100 Oe suggests very good AP alignment, while the nearly saturated magnetization observed at +100 Oe indicates good P alignment. Similarly, well-defined alignment of the P and AP states can be achieved at temperatures in and below the superconducting transition.

Measurements of  $T_c^P$  and  $T_c^{AP}$  were performed by alternating the applied field between +100 and -100 Oe, while the temperature was slowly decreased through the transition region. The largest shift in critical temperature,  $\Delta T_c \equiv T_c^{AP} - T_c^P$ , should occur in samples with the Nb thickness close to  $d_s^{cr}$ . The inset to Fig. 1 shows a plot of  $R$  vs.  $T$  for a sample with a nominal thickness  $d_s = 21.5$  nm, measured in a dilution refrigerator, with a  $T_c = 1.42$  K. Two distinct transitions are observed for P and AP alignment, with a separation in temperature  $\Delta T_c \approx 9$  mK for this case. Samples with  $d_s \approx 22$  nm have  $T_c$ 's between 2 and 3 K and exhibit values for  $\Delta T_c$  of only a few mK, similar to results obtained previously in other F/S/F systems.<sup>11,12,13</sup> There is no observable difference between the P and AP state for samples with  $d_s > 26$  nm.

Figure 3 shows a plot of  $\Delta T_c$  vs.  $T_c$  for nine samples. The largest observed  $\Delta T_c$  for our Py/Nb/Py trilayers is about 20 mK for a sample with  $d_s = 20.5$  nm and  $T_c = 0.385$  K. The data are somewhat scattered for the thinnest Nb layers due to the increased sensitivity of  $T_c$  to small variations of thickness and growth conditions. Nonetheless, our samples always show that  $T_c^P < T_c^{AP}$ , a result that is opposite to what was observed by Rusanov *et al.*<sup>14</sup> in similar Py/Nb/Py trilayer systems.

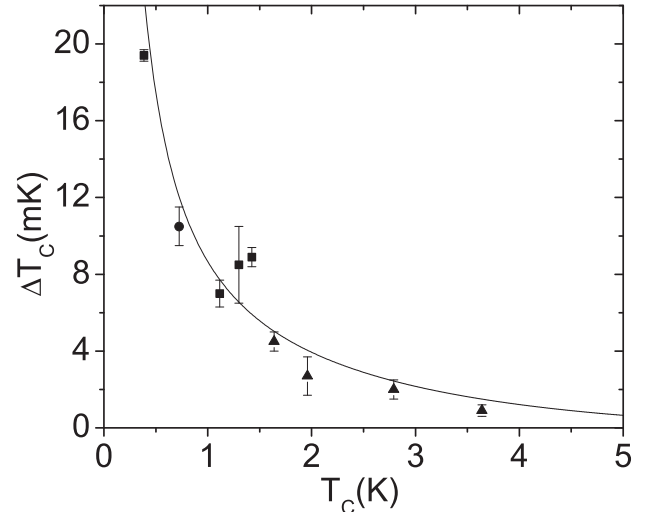


FIG. 3:  $\Delta T_c$  vs. critical temperature for a series of  $\text{Py}(8)/\text{Nb}(d_s)/\text{Py}(8)/\text{Fe}_{50}\text{Mn}_{50}(8)/\text{Nb}(2)$  illustrating the difference in  $T_c$  between the P and AP state. The fit to the data is obtained using the theory of Fominov *et al.*<sup>21</sup> as outlined in the text.



The critical temperature of F/S/F trilayers in the P and AP states has been calculated theoretically by several groups.<sup>8,9,21,22,23</sup> The usual approach involves solving the Usadel equations in the dirty limit, which for the superconductor implies  $l_S < \xi_{BCS} = \hbar v_S \gamma / \pi^2 k_B T_{c0}^b$ , and for the ferromagnet  $l_F < \hbar v_F / E_{ex}$ , where  $l_S$  and  $l_F$  are the electron mean free paths in S and F. Here,  $T_{c0}^b$  is the transition temperature of the bulk superconductor,  $v_S$  and  $v_F$  are the Fermi velocities in the S and F materials, and  $\gamma = 1.7811$ . These simplified theories do not consider different electronic properties for the majority and minority spin bands of the F material.

We compare our data with the theory of Fominov *et al.*<sup>21</sup> The following equations, which describe the critical temperatures  $T_c^P$  and  $T_c^{AP}$  for the P and AP cases, are obtained in the limit of a thin S layer with a constant superconducting gap  $\Delta$ , and a strong ferromagnet with  $E_{ex} \gg \Delta$ :

$$\ln \frac{T_{c0}}{T_c^P} - Re \Psi \left( \frac{1}{2} + \frac{V_h \xi_S T_{c0}}{2 d_s T_c^P} \right) + \Psi \left( \frac{1}{2} \right) = 0 \quad (1)$$

$$\ln \frac{T_{c0}}{T_c^{AP}} - \Psi \left( \frac{1}{2} + \frac{W \xi_S T_{c0}}{2 d_s T_c^{AP}} \right) + \Psi \left( \frac{1}{2} \right) = 0, \quad (2)$$

where  $\xi_S = \sqrt{\hbar D_S / 2\pi k_B T_{c0}}$  and  $T_{c0}$  is the critical temperature for an isolated superconducting layer of thickness  $d_s$ . Fominov *et al.* make the important point that the existence of a significant dependence of  $T_c$  as a function of the relative magnetization angle for  $d_s > \xi_S$  is due to the fact that the critical temperature of the trilayer is suppressed as compared to that of the isolated Nb layer, i.e.  $T_c \ll T_{c0}$ . Consequently, the condition for which this theory is valid,  $d_s \ll \xi = \sqrt{\hbar D_S / (2\pi k_B T_c)}$ , is considerably weaker than the condition  $d_s \ll \xi_S$ , because  $\xi \gg \xi_S$ . In the limit of thick ferromagnets, the  $\tanh$  functions in ref.<sup>21</sup> are set to 1, and the functions  $V_h$  and  $W$  in Eqns. 1 and 2 become

$$V_h = \frac{\rho_S \xi_S}{(1-i)\rho_F / 2k_h + R_{BA}} \quad W = Re\{V_h\} \quad (3)$$

where  $k_h = \sqrt{E_{ex} / \hbar D_F}$  is the inverse coherence length in F and  $R_{BA}$  is the boundary resistance times area of the S/F interface, a parameter whose value reflects both the quality of the interface and the Fermi surface mismatch between the S and F materials. Eqns. (1-3) produced the fits to the Py/Nb/Py data shown in Fig. 1 and 3.

Estimates for the parameters appearing in the theory were obtained by performing additional measurements on bulk and thin film samples. Since the F layer is treated in the thick limit and its thickness remains fixed for all our samples, we have used a bulk value for the resistivity of Py, namely  $\rho_F = 123 \text{ n}\Omega \text{ m}$ .<sup>24</sup> By contrast, the thickness of the S layer in our trilayers changes, and thus we have measured  $\rho_S$  as a function of the thickness on bare Nb thin films. In addition, the variation of  $T_{c0}$  with thickness was also measured on the same Nb films. The explicit dependencies of  $\rho_S$  and  $T_{c0}$  were taken into account

in Eqns. 1 and 2.<sup>25</sup> The coherence length was obtained by performing perpendicular field measurements on the bare Nb films, giving  $\xi_S \approx 6 \text{ nm}$  in the thickness range of our data. Taking the limit of  $T_c \rightarrow 0$  in Eq. 1, for the behavior as  $d_s$  approaches the critical thickness  $d_s^{cr}$ , results in the relation  $d_s^{cr} / \xi_S = 2e^C |V_h|$  where  $C = 0.577$  is the Euler constant. Using this constraint in Eq. 3 one can obtain an estimate for the boundary resistance:

$$R_{BA} \approx 2e^C \rho_S (d_s^{cr}) \frac{\xi_S^2}{d_s^{cr}} \quad (4)$$

where the value of  $\rho_S$  is taken at the critical thickness. After constraining  $R_{BA}$  as shown above and using the measured values for the resistivities and  $\xi_S$ ,  $k_h$  is the only remaining fit parameter.

Using Eq. 4 with  $d_s^{cr} = 20.5 \text{ nm}$  and  $\xi_S = 6 \text{ nm}$  gives the estimate  $R_{BA} = 1.5 \text{ f}\Omega \text{ m}^2$ , which when utilized in Eq. 1 yields a fit that follows the  $T_c$  vs  $d_s$  data very well, as shown in Fig. 1. The fit to the  $T_c$  vs  $d_s$  data is somewhat insensitive to the value of  $k_h$ , however. That parameter is tightly constrained by fitting to the  $\Delta T_c$  vs  $T_c$  data. The results of that fit are illustrated in Fig. 3, showing good agreement to the data with  $k_h = 1.0 \text{ nm}^{-1}$ . In comparison, independent estimates of  $k_h$  using the values of  $v_F$  and  $l_F$  discussed earlier are  $0.8$  and  $2.0 \text{ nm}^{-1}$  for the majority and minority spin bands, respectively.<sup>18</sup>

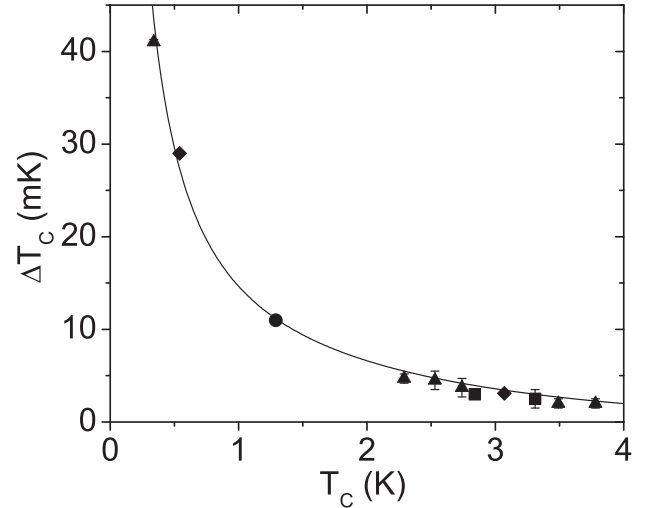


FIG. 4:  $\Delta T_c$  vs. critical temperature for a series of Ni(7)/Nb( $d_s$ )/Ni(7)/Fe<sub>50</sub>Mn<sub>50</sub>(8)/Nb(2).<sup>13</sup> The fit to the data is obtained using the theory of Fominov *et al.*<sup>21</sup>

The excellent fit shown in Fig. 3 motivated us to apply the theory of Fominov *et al.* to our previously-reported data on Ni/Nb/Ni trilayers.<sup>13</sup> The results of the fit to the  $\Delta T_c$  vs  $T_c$  data from the Ni/Nb/Ni trilayer are illustrated in Fig. 4, and also show excellent agreement, even though it is not obvious *a priori* that the Ni layers in those samples are in the dirty limit. The values  $\rho_F = 33 \text{ n}\Omega \text{ m}$ ,  $\xi_S = 6 \text{ nm}$  and  $d_s^{cr} = 16.5 \text{ nm}$  were used in the fit, which gave  $R_{BA} = 2.3 \text{ f}\Omega \text{ m}^2$  for the



Ni/Nb interface and  $k_h = 0.5 \text{ nm}^{-1}$ . We have made independent measurements of the Nb/Ni interface resistance using current-perpendicular-to-plane resistance measurements of Nb/Ni multilayers, and find the value  $R_B A = 2.35 \pm 0.25 \text{ f}\Omega \text{ m}^2$ , in excellent agreement with the value obtained from the fit to the  $T_c$  vs.  $d_S$  data. Our independent estimate of  $k_h$  varies over a broad range due to uncertainty in determining the value of the diffusion constant (or mean free path) in Ni.<sup>13</sup> From the measured resistivity, we obtain values of  $l_F$  ranging between 7 and 70 nm, depending on what value we take for the product  $\rho_F l_F$  for Ni.<sup>26</sup> Combining that with the values for the exchange energy  $E_{ex} = 0.115 \text{ eV}$  and the Fermi velocity  $v_F = 0.28 \times 10^6 \text{ m/s}$ ,<sup>17</sup> we obtain values for  $k_h$  ranging from  $0.16 - 0.5 \text{ nm}^{-1}$ . The value corresponding to the shorter  $l_F$  agrees with the value from the fit to the data in Fig. 4.

The question remains open as to why Rusanov *et al.*<sup>14</sup> observe inverse spin switch behavior,  $T_c^P > T_c^{AP}$ , whereas we observe the standard behavior,  $T_c^P < T_c^{AP}$ . The most obvious difference between our samples and theirs is that we use exchange bias to pin the magnetization direction of one Py layer, whereas they rely on the different coercivities of the two layers. But the switching data in their micron-scale samples show a clear plateau, which suggests that they have achieved a good AP magnetization configuration. A second comment is that they observe a difference between  $T_c^P$  and  $T_c^{AP}$  even when the

Nb layer is very thick, 60 nm, whereas sensitivity to the ferromagnet orientation is limited to our samples with  $d_s < 28 \text{ nm}$ . Variations in resistance or  $T_c$  have also been observed in F/S bilayers due to domain formation during magnetization switching.<sup>27,28</sup> But Rusanov *et al.* state that the features indicating the inverse spin switch effect in their trilayers were not observed in bilayers. This fact, combined with their data in micron-scale samples that appear to be single-domain, argue against any role of domains in producing the inverse effect.

In summary, we observe similar spin-switch behavior in Py/Nb/Py and Ni/Nb/Ni trilayers – both S/F systems with strong ferromagnets. The results from both systems are fit well with the dirty-limit Usadel theory of Fominov *et al.*<sup>21</sup> This success is somewhat unexpected given that this oversimplified theory assumes identical electronic properties (density of states, Fermi velocity, and mean free path) for the majority and minority spin bands of the ferromagnetic material, whereas Py is known to have a strong spin-scattering asymmetry. The success of a dirty-limit theory in Ni is also surprising, and may be due partly to strong diffusive scattering of electrons from the S/F interfaces.

We are grateful to J. Bass, R. Loloe and A. Rusanov for fruitful discussions. This work was supported by NSF grants DMR 9809688, 0405238 and 0501013 and by the Keck Microfabrication Facility.

- 
- \* Electronic address: birge@pa.msu.edu
- <sup>1</sup> For a review, see Yu.A. Izyumov, Yu.N. Proshin, and M.G. Khusainov, *Phys.-Uspekhi* **45**, 109 (2002).
  - <sup>2</sup> J.S. Jiang, D. Davidovic, D.H. Reich, and C.L. Chien, *Phys. Rev. Lett.* **74**, 314 (1995).
  - <sup>3</sup> L.V. Mercaldo *et al.*, *Phys. Rev. B* **53**, 14040 (1996).
  - <sup>4</sup> Th. Mühge *et al.*, *Phys. Rev. Lett.* **77**, 1857 (1996).
  - <sup>5</sup> T. Kontos, M. Aprili, J. Lesueur, and X. Grison, *Phys. Rev. Lett.* **86**, 304 (2001).
  - <sup>6</sup> V.V. Ryazanov *et al.*, *Phys. Rev. Lett.* **86**, 2427 (2001).
  - <sup>7</sup> P.G. DeGennes, *Phys. Lett.* **23**, 10 (1966).
  - <sup>8</sup> L.R. Tagirov, *Phys. Rev. Lett.* **83**, 2058 (1999).
  - <sup>9</sup> A.I. Buzdin, A.V. Vedyayev, and N.V. Ryzhanova, *Europhys. Lett.* **48**, 686 (1999).
  - <sup>10</sup> G. Deutscher and F. Meunier, *Phys. Rev. Lett.* **22**, 395 (1969).
  - <sup>11</sup> J.Y. Gu *et al.*, *Phys. Rev. Lett.* **89**, 267001 (2002).
  - <sup>12</sup> A. Potenza and C.H. Marrows, *Phys. Rev. B* **71**, 180503(R) (2005).
  - <sup>13</sup> I.C. Moraru, W.P. Pratt Jr., N.O. Birge, *Phys. Rev. Lett.* **96**, 037004 (2006).
  - <sup>14</sup> A. Yu. Rusanov, S. Habraken, J. Aarts, *Phys. Rev. B* **73**, 060505(R) (2006).
  - <sup>15</sup> V. Peña *et al.*, *Phys. Rev. Lett.* **94**, 057002 (2005).
  - <sup>16</sup> S. Takahashi, H. Imamura, and S. Maekawa, *Phys. Rev. Lett.* **82**, 3911 (1999).
  - <sup>17</sup> D.Y. Petrovykh *et al.*, *Appl. Phys. Lett.* **73**, 3459 (1998).
  - <sup>18</sup> K.N. Altmann *et al.*, *Phys. Rev. Lett.* **87**, 137201 (2001) report the mean free paths for the majority and minority spin bands in Ni<sub>90</sub>Fe<sub>10</sub> and Ni<sub>80</sub>Fe<sub>20</sub>. Interpolating between these two alloys, one finds approximately  $l_F^\downarrow = 0.6 \text{ nm}$  and  $l_F^\uparrow > 3 \text{ nm}$ . From the spin scattering asymmetry in Py,  $\beta = 0.73$ ,<sup>19</sup> we expect  $l_F^\uparrow/l_F^\downarrow = (1 + \beta)/(1 - \beta) = 6.4$ . Using  $l_F^\downarrow = 0.6 \text{ nm}$  gives  $l_F^\uparrow = 4 \text{ nm}$ , which is consistent with the measured lower limit.
  - <sup>19</sup> S.D. Steenwyk *et al.*, *J. Magn. Magn. Mater.* **170**, L1 (1997).
  - <sup>20</sup> J. Nogués and I.K. Schuller, *J. Magn. Magn. Mater.* **192**, 203 (1999).
  - <sup>21</sup> Ya.V. Fominov, A.A. Golubov, and M.Yu. Kupriyanov, *JETP Lett.* **77**, 510 (2003).
  - <sup>22</sup> I. Baladié and A. Buzdin, *Phys. Rev. B* **67**, 014523 (2003).
  - <sup>23</sup> C.-Y. You *et al.*, *Phys. Rev. B* **70**, 014505 (2004).
  - <sup>24</sup> W.P. Pratt *et al.*, *J. Appl. Phys.* **79**, 5811 (1996).
  - <sup>25</sup> In the thickness range of our data, the resistivity of bare Nb films varies as  $\rho_S[\text{n}\Omega \text{ m}] = 99 + 3415/d_s[\text{nm}]$ , while that of the bare critical temperature is  $T_{c0}[\text{K}] = 9.1 - 43/d_s[\text{nm}]$ .
  - <sup>26</sup> Using the Einstein relation,  $\rho = (n(E_F)De^2)^{-1}$ , with  $v_F = 0.28 \times 10^6 \text{ m/s}$ <sup>17</sup> and  $n(E_F) = 1.77 \times 10^{48} \text{ J}^{-1} \text{ m}^{-3}$  from J.W.D. Connolly, *Phys. Rev.* **159**, 415 (1967), we find  $\rho_F l_F = 0.24 \text{ f}\Omega \text{ m}^2$ . C. Fierz *et al.*, *J. Phys. Condens. Matter* **2**, 9701 (1990) give  $\rho_F l_F = 0.7 - 2.3 \text{ f}\Omega \text{ m}^2$ .
  - <sup>27</sup> A. Yu. Rusanov, M. Hesselberth, J. Aarts, and A.I. Buzdin, *Phys. Rev. Lett.* **93**, 057002 (2004).
  - <sup>28</sup> R.J. Kinsey, G. Burnell, and M.G. Blamire, *IEEE Trans. App. Supercond.* **11**, 904 (2001).